Dear Handling Editor Oliver Gagliardini and Anonymous Reviewers,

Thank you for the time you have invested in my manuscript. I have attempted to improve the manuscript following the comments provided below (my responses are in green).

Sincerely,

Brad Lipovsky

Response to Reviewer #3

The paper suffers however, to my point of view, of a lack of accuracy in the presentation of the model used and on the assumptions that are made. A mixture of too complicated vocabulary (and to my point of view not necessary) and not enough explanation of simple notions make the paper very difficult to follow and read.

As scientists and writers, we are often faced with the challenge of using precise and accurate vocabulary while at the same time trying to keep things as simple as possible. I've taken the reviewer's comments to heart and made an honest effort to simplify the language in the paper and to improve the structure (the latter discussed in detail further on). I believe that the exposition has significantly benefitted from these changes. I have attempted to addressed this concern throughout the manuscript by specifically responding to the following points.

Furthermore, the paper would be very much improved by adding more detailed comparison with rift propagation and ice-shelf stability in the field where I expect measurements have been made.

This is an excellent point. I have recently undertaken a systematic effort aimed at ice shelf rift observation. This is still work in progress. Unfortunately, at the present time, the extremely simplistic model geometry that we use makes it difficult to directly compare our model to observations. I therefore have the opinion that comparison with observations is best left at a relatively qualitative level. A note to this extent has been provided in the manuscript. That being said, the discussion does provide several points of comparison with ice shelf rifts. I specifically discuss observations surrounding the role of mélange as well as the seismic observations made by Lipovsky (2018). The present study has demonstrated that geometrical effects are quite important during rift propagation. For this reason, I do think that more detailed comparisons are better left for a modeling study that deals with a more realistic ice shelf geometry.

I detail below the points that have to be clarified:
0 - Abstract:
L4-5: The sentence is not clear: '… near-tip rift walls'.

I have simplified this sentence.

L6-7: It is not obvious by reading just the abstract to understand '….advection of rifts … may trigger rift propagation'. In particular what does mean 'advection of rift' ? How is it different from rift propagation? This has to be more clearly stated for readers that are not exactly in the field.

I have simplified this language.

More generally, when reading the last sentence, it seems that there is no other studies on the description of calving physics based on fracture mechanics. It seems however to me that other studies have been done in this direction.

I have changed this sentence.

1- Introduction

In the introduction, discussion and conclusion, there is a lack of detailed description of what is observed on the field related to the study performed in this paper. Furthermore, there is a lot of work based on fracture mechanics that have been done in rock mechanics and also in rupture propagation for earthquakes. Because no references related to this work are present in this paper, it seems that the author is not aware of it, making it difficult to situate his work compared to the state of the art in the domain.

I have significantly changed the ordering of ideas presented in the introduction. Some material has been moved to Section 4. As previously written, the paper introduces only fracture mechanical studies of ice shelf rifts in the introduction section. I decided not to clutter the introduction with fracture mechanical detail. The interested reader will note the extensive discussion of classical fracture mechanics later in the paper, at the point where fracture mechanics is introduced.

2 – Background

One of the main problem of this paper is that the equations and hypothesis used are not clearly presented. At the beginning of the background section, simple equations described by complicated words are presented.

I agree that this section of the paper was confusing. For this reason, I have restructured this section, mostly by moving existing text to different parts of the paper. In that way, the same information is conveyed but in a more logical order. In the new manuscript, I now make it clear that the equations previously in Section 2 are only used in the two-dimensional model. For this reason, these equations are now given in the newly-created Section 4, dedicated exclusively to describing the two-dimensional model.

First, equation (1) is related to the hydrostatic approximation for the pressure taking into account buoyancy but is referred to as 'in-plane horizontal membrane stress'. While I assume that the author refer to the shallow ice approximation, the use of such words do not provide clear description of the approximation made at least for researchers that are not specialists of the ice-shelf and rift problem.

Just to be clear, the model is not related to the shallow ice approximation (SIA) model. The two dimensional model is more similar to a shallow shelf approximation (SSA) model, but it does not assume incompressibility as does SSA. The term membrane stress is widely used in modern ice sheet modeling and its use here is consistent with that literature. I believe that the confusion surrounding this topic should be alleviated by having moved this material to a later section, as described above.

To make the considered forces clear, I suggest to draw the forces involved in Figure 1 or Figure 2.

The reviewer proposes an interesting idea to create additional diagrams illustrating the balance of forces. Because of the way that the paper has been restructured, I'm not sure that this is necessary. Furthermore, such figures are given in standard references (i.e., Macayeal). As it is currently written the manuscript contains two diagrammatic figures (1A and 1B). For these reasons, I do feel that an additional diagrammatic figure is not warranted.

Because the cryosphere readers are not all aware of the way you calculate the balance of forces, this should be clearly recalled as it is the basis of this paper.

I have added a sentence to this effect in Section 4, where the depth-integrated membrane stress is now first stated.

I don't understand why the author used the symbol ≙ that he refers to 'a definition'. Equation (1) is not a definition, it represents the normal stress under some approximations. Again, this kind of things complicate the problem for nothing (at least I don't see what information it provides to the reader) and is very strange when put in regards to the very simple approximations, equations, and approach used here (with no demonstration, etc.).

This confused another reviewer as well, so I've gotten rid of all occurrences of the three-line equality symbol.

L 58: Demonstrate how to you express the bending moment leading to equation (3) (use a figure if necessary).

First, please note that this equation is now placed in Section 4 as Eq. 21. I am not completely sure what the reviewer means by "express." The new context in Section 4 may provide a better

expression of the meaning of this equation. The calculation of moments is carried out in the classic paper by Reeh. Given that the manuscript under consideration already on the long side, it is my opinion that explicitly presenting the derivation or figures regarding the ice front moment expressions would not significantly improve the manuscript.

L66: show in the figure 1b what you state in the text.

I have now made the language in the text match the language in the figure.

L72: There should be studies on 3D effects on rupture propagation in Earthquake or rock mechanics that should be recalled here.

For reference, the old line 72 stated, "Although a number of previous studies have examined ice shelf rifts using LEFM, no previous study appears to have considered three-dimensional effects." Note that later on in the paper, extensive reference is given to background material in fracture mechanics. Concerning the point presented here, yes, there is a large literature on 3D effects in earthquake rupture dynamics. The 3D effects in ice shelves, however, are quite different because ice shelves, as the manuscript demonstrates, have strong interactions with buoyancy. These effects are absent during, for example, tectonic earthquake rupture. Furthermore, earthquake rupture tends to involve rupture front propagation at a substantial fraction of the elastic wave speeds. Fracture propagation at this rate is drastically different than the quasi-static propagation considered here. Given that this connection is sufficiently distant, it seems preferable to not draw this connection.

Figure 1 : It is difficult to make the link between Figure 1A and Figure 1B. To avoid getting lost, the author could draw the flow direction in each sub-figures of Figure 1 and 2. The orange arrow associated to 'Top-out rotation' correspond to me to 'Bottom-out' rotation for calving. What is the point here ? Represent the rift tip on the figure. Legend of Figure 1B: I don't see on the figure what is stated in the legend 'Zoomed in view of an ice shelf rift tip showing how buoyancy driven rotation of the rift walls results in partial contact of the rift walls near the rift tip'. Define in the text or in the legend how the flexural gravity wavelength is calculated.

I have attempted to address these issues. First of all, I have added a reference to the equation where the flexural gravity wavelength is defined in the figure caption. Concerning the definition of top-out versus bottom out, I would argue that this is why it is important to define terms. This usage of the term makes sense to me: the top of the ice shelf moves outwards away from the ice. Perhaps there is some confusion because the top moves towards the center of the rift. In that way the definition is arbitrary and I would argue that as long as the usage is consistent then the choice is unimportant. The term top out is used self consistently within the manuscript and is consistent with sense of rotation drawn in the figure. Given this self-consistency I do not believe that any change is warranted.

3 – Mechanical model

What is the link between the background section and the model used here ?

This question highlights the lack of clarity surrounding the relationship between the full three-dimensional and the simplified two-dimensional model. Based on this comment, I have opted to move part of the background material into the later section about the two dimensional model, as discussed previously.

Why two different L are chosen for the marginal and central rifts. It makes the message unclear as the role of L may be important in the different behavior of the marginal and central rifts. Could you explain your choice and could you do the analysis by comparing marginal and central rifts for the same L ?

This is a standard convention in fracture mechanics, to define fractures in a whole space in terms of their half-length but to define edge fractures in terms of their entire lengths. This convention stems in part from analytical solutions for simplified geometries. The usage in the manuscript is consistent with standard stress intensity factor handbooks such as Tada (2000) and for this reason I would argue against making the suggested change.

L 97-101 : This is not clear, illustrate on a figure.

The actual crack tip region used in the simulations is shown in Figure 2 and a curved crack tip is shown in Figure 1b. A note has been made about this.

L 100: Show in the appendix the sensitivity to the choice of the width because it is not obvious how much its influence is negligible.

This is a good point. I have added a note (in the main text, Section 2.1) describing the influence of changing the rift width. I point out that changing the rift width by 50% results in a ~1% change in the resulting SIFS.

L 100-101: Give more details about what you do when you refer to ‘tapering’.

This language was out of date; the rectangle is not tapered.

Equation (5): You forget the Identity tensor. Same L 116.

I have made this change.

Equation (6): What is H ? Is it h in Figure 1 ? Then the same notation should be used. H is not constant when there is a rift so that the horizontal pressure gradient could not be neglected when replacing T’ by T ? As a result, equation (7) is not obtained. Maybe I missed something but all this should be made clearer.

Thank you for pointing this out, this symbol was not defined previously! H is the ice shelf surface height. H remains constant even though H is not defined in the rift For this reason (old) equation 7 remains valid.

Equation (10): As you makes a variable change and use T instead of T', the boundary conditions should be expressed in terms of T too.

Yes, that's correct that the boundary conditions change. All of the terms in the new boundary conditions have been written out already, and since the new boundary conditions are more complicated I do not think it is necessary to write out the new boundary conditions. It is an important point, however, and so I have made a note to this extent in order to draw the reader's attention to this detail.

L 135: relate the displacement vector to u_i, u_j, …

I have made this change.

Figure 2: The flow direction should be added here too.

I have made this change.

L 145-146: What are the boundary conditions used in the 3D calculations then ?

This sentence was confusing so I removed it. The 3d boundary conditions are now clearly stated.

L 150 : recall what is 'free' (triangular mesh)

I have clarified this point.

Equations (12)-(14) Recall the hypothesis made to obtain these equations

It's a surprising fact about LEFM that all of the conditions were in fact already stated: simply that a sharp fracture be located in a loaded elastic solid. There is nothing else to be stated.

L 200: It is not clear how do you calculate them.

On this topic, I refer the interested reader to the citations given.

L 260: It could be good to show it on a figure.

This is a minor point in the paper and I do not think it warrants an additional figure.

5 - Discussion: The main problem of the discussion is that the results are not enough compared with field observation.

Please note the response I made to the second comment in the review. I would furthermore argue that I do compare to the field observations described by Lipovsky (2018). These are seismic observations from which inferences were made about stress intensity factors. I also discuss the field observations made by Olinger et al. (2019). While I agree that additional and more detailed comparisons would be interesting, these two comparisons do form a good basis for an evaluation of the model predictions.

L 299-301: Put marks on Figure 6 to show what is stated in the text.

This was already shown in the figure although the confusion indicates that the labelling was not sufficiently clear. I have improved the text in this regard.

L 304-305 and L 308-309 are not clear.

I have rewritten these statements.

6 - Conclusion: This should recall the assumptions made in the model and summarize the results, the limitation of the approach and the comparison with field observation.

I disagree, as this was already done at the beginning of the Discussion section and the choice of one location over the other seems purely aesthetic.

Ice shelf rift propagation: stability, three-dimensional effects, and the role of marginal weakening

Bradley Paul Lipovsky

Department of Earth and Planetary Sciences
Harvard University

Correspondence: brad_lipovsky@fas.harvard.edu

Abstract. Understanding the processes that govern ice shelf extent are ~~of fundamental importance to improved~~ important to improving estimates of future sea-level rise. In present-day Antarctica, ice shelf extent is most commonly determined by the propagation of through-cutting fractures called ice shelf rifts. Here, I present the first three-dimensional analysis of ice shelf rift propagation. I ~~present a~~ model rifts using the assumptions of linear elastic fracture ~~mechanical~~ mechanics (LEFM)~~description of rift propagation~~. The model predicts that rifts may be stabilized (i.e., stop propagating) when buoyant flexure results in ~~contact at the tops of~~ the ~~near-tip~~ partial contact of rift walls. This stabilizing tendency may be overcome, however, by processes that act in the ice shelf margins. In particular, ~~both marginal weakening and the advection of rifts into an ice tongue are shown to be processes that may trigger rift propagation. Marginal shear stress~~loss of marginal strength, modeled as a transition from zero tangential displacement to zero tangential shear stress, is shown to ~~be the determining factor that governs these types of rift instability. I furthermore~~ favor rift propagation. Rift propagation may also be triggered if a rift is carried with the ice flow (i.e., advected) out of an embayment and into a floating ice tongue. I show that rift stability is closely related to the transition from uniaxial to biaxial extension known as the compressive arch. Although the partial contact of rift walls is fundamentally a three-dimensional process, I demonstrate that it may be parameterized within more numerically efficient two-dimensional calculations. This study ~~provides~~ constitutes a step towards a ~~description of calving physics that is based in fracture mechanics~~first-principles description of iceberg calving due to ice shelf rift propagation.

1 Introduction and background

~~The Antarctic ice sheet is projected to loose mass this century.~~ Despite decades of progress, it remains unclear whether Antarctica will gain or lose mass by the year 2100. Although the rates of mass ~~loss~~ change over this timeframe are typically projected to ~~mirror recent rates~~be nearly linear (**??**), several types of more extreme ice sheet response to global climate forcing cannot presently be excluded~~(?)~~. Perhaps the most prominent of these extreme changes is the retreat of the floating ice shelves that fringe the Antarctic continent. Ice shelf retreat has been observed to occur gradually, i.e., over a period of years to decades (**??**), and also abruptly, i.e., over a period of weeks to months (**??**). Although ice shelves ~~themselves do not~~ are floating and therefore do not directly contribute to sea-level rise, they do act to buttress grounded ice (**????**). For this reason, ice sheet mass and therefore global mean sea-level are closely connected to the extent and stability of ice shelves. Here, I examine the stability of ice shelves with respect to the propagation of large through-cutting fractures called rifts.

The largest modern ice shelves exist in coastal embayments. This basic observation has long prompted the notion that embayments ~~promote the existence of large stable ice shelves (????). Yet not all ice shelves fully~~ stabilize ice shelves (**???**). Yet the exact relationship between coastal geometry and ice shelf extent is not trivial. For example, ice shelves do not generally fill the largest possible embayment ~~. The~~ in the way that the Ross and Amery Ice Shelves do. Instead, ice shelves such as the Pine Island Glacier Ice Shelf ~~, for example, does not presently fill the entire embayment~~ are limited to much smaller local embayments (in the case of Pine Island, the present-day ice shelf extends to Evans Knoll rather than the entire region between Bear Peninsula and Thurston Island~~; instead it fills the much smaller local embayment of Pine Island Bay~~). Furthermore, analysis of sediment cores (**??**) and ~~iceberg scour marks (?)~~ various bathymetric features (**??**) suggest that past ice shelves have waxed and waned in extent through ice age cycles. Although ~~embayments~~ coastal embayments do appear to stabilize ice shelves, it would ~~therefore~~ also appear that some other process is responsible for determining the ~~size~~ extent of a stable ice shelf within a given coastal geometry. The close relationship between the state of stress in an ice shelf and the ice shelf boundary conditions (**???**) motivates investigation into processes acting in ice shelf margins.

Ice shelf margins are the part of the ice shelf grounding zone that is roughly parallel to flow (see Fig. 1). The importance of ice shelf margins is suggested by several observations, foremost among these being the observation of marginal weakening prior to ice shelf collapse. Estimates of ice rheology based on the inversion of surface velocity fields show extensive marginal weakening prior to the collapse of the Larsen A (**?**) and Larsen B Ice Shelves (**??**). Although ice shelf collapse (i.e., total and rapid retreat) is a complex phenomenon that involves other processes besides rift propagation ~~(?)~~(**??**), rift propagation does appear to play a role in collapse. **?** explicitly noted that marginal weakening immediately preceded rift propagation and eventual collapse on Larsen B. Further observation of a relationship between ice shelf retreat, rifting, and marginal thinning has been noted in the Amundsen Sea Embayment (**?**) and Jakobshavn Isbrae, Greenland (**?**). Motivated by these observations, a central question of this paper is, what is the precise mechanical relationship between ice shelf margins and ice shelf rift propagation?

~~The main result~~ One of the main glaciological results of this paper is that marginal weakening can destabilize rift propagation. ~~I begin by providing background on the state of stress in an ice shelf in Sections ??. In Section 2 I describe three-dimensional elasticity calculations that are carried out using the finite element method and then post-processed to reveal fracture mechanical~~

properties. A more precise statement of the main result is then given in Section 3, where I also examine a simplified analytical treatment of the three-dimensional calculations. I conclude by discussing the relationship between rift propagation, the compressive arch, rift-filling melange, and ocean swell in Section 6.

2 Background

I consider an ice shelf to be a buoyantly floating elastic plate of uniform thickness. Stress balance at the seaward-facing ice front results in both a net bending moment and an in-plane horizontal membrane stress (**??**). The vertically-averaged membrane stress is,

$$\sigma_m \equiv \frac{\rho g h}{2}\left(1 - \frac{\rho}{\rho_w}\right).$$

I use the $\equiv$ symbol to denote a definition. The bending moment is given by,

$$m_0 \equiv \frac{\rho g h^3}{12}\left[3\left(\frac{\rho}{\rho_w}\right) - 2\left(\frac{\rho}{\rho_w}\right)^2 - 1\right] \equiv \phi\frac{\rho g h^3}{12}.$$

In these expressions, ρ An investigation into the forces that drive rift propagation requires a careful accounting of the forces acting on the rift walls. **?** was the first to document how a freely floating ice front experiences a net torque due to an imbalance between the overburden pressure in the ice and ρ_w are the densities of ice and water and h is the ice thickness. Typical values of $\rho/\rho_w = 0.90$ give $\phi = 0.08$. The bending moment may also be expressed as a bending stress,

$$\sigma_b \equiv \frac{6 m_0}{h^2} = \phi\frac{\rho g h}{2}.$$

The bending stress σ_b is the value of the rift-normal stress at the top of the ice shelf; it is also the maximum value of the rift-normal stress. The horizontal component of loading (Eq. 18) is commonly used as a boundary condition in numerical ice flow models, whereas the bending moment is not typically applied in ice sheet models because its effects are confined to a narrow boundary layer in the vicinity the hydrostatic water pressure. This torque is expected to cause a rotation of the ice front (**?**).

with a top-out sense of motion (**?**). Rifts walls have the same ice-front boundary conditions as a seaward-facing ice front and are therefore expected to experience a similar rotation. The main difference between a seaward-facing ice front and a rift wall is that it is possible for rift walls to come into contact. This contact is expected to occur at the top of the ice shelf and in the region near the rift tip, as illustrated in Fig. 1b. Indeed, This behavior has been observed in the field. **?** recently observed that a rift tip on the Brunt Ice Shelf was further advanced at depth than at the surface, suggesting the occurrence of partial contact. I examine the partial contact of rift walls in Section 3. As an aspect of linear elastic fracture mechanics, fracture wall contact is a well-studied topic (**?**, Chapter 1, Section C).

I use three-dimensional elasticity calculations combined with model rifts using linear elastic fracture mechanics (LEFM)to examine the propagation of ice shelf rifts. Although a number of previous studies have examined ice shelf rifts using LEFM,

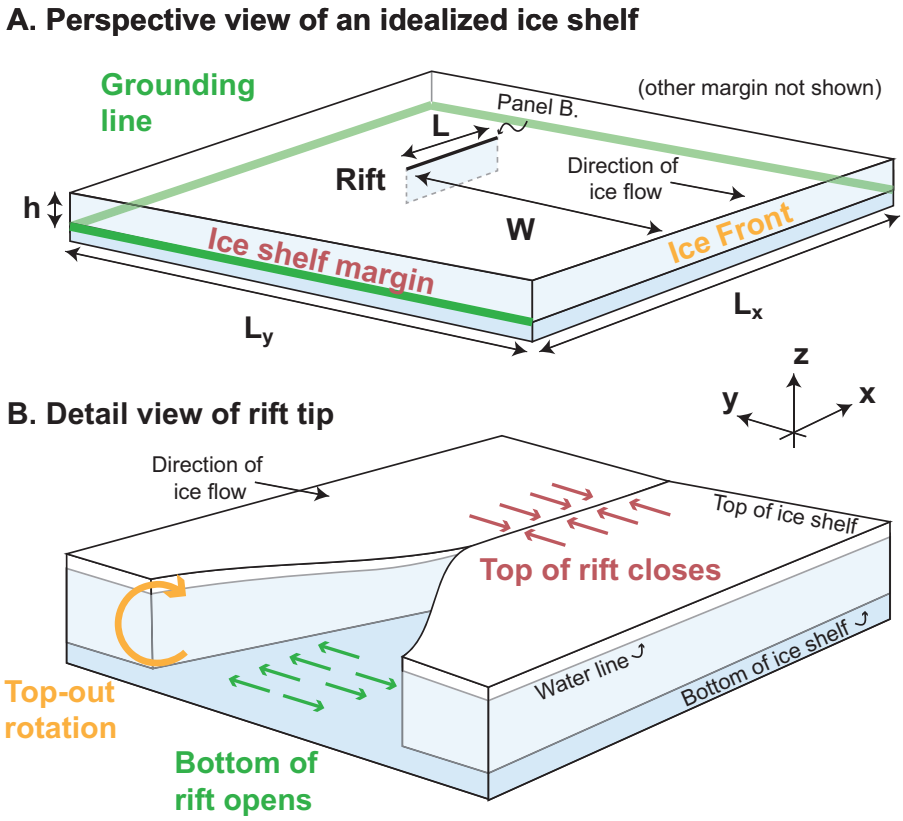

Figure 1. A. ~~Simplified geometry of an idealized rectangular ice~~ Ice shelf ~~.~~ geometry used in this study. B. ~~Zoomed in view~~ View of ~~an ice shelf~~ rift tip showing ~~how buoyancy-driven rotation of the rift walls results in~~ partial contact of ~~the~~ rift walls ~~near the rift tip. Note that B. is~~ (drawn ~~under the assumption that the rift tip is at least several flexural gravity wavelengths away from the ice shelf margin so that no flexural interaction occurs between these two regions.~~assuming distant margins)

no previous study appears to have considered three-dimensional effects. **?** calculated two-dimensional mixed mode (in-plane opening and shearing) stress intensity factors and as a result was able to state a fracture condition as well as predict rift propagation paths. Other ice shelf LEFM studies have mostly focused on propagation paths (**???**) and near-tip deformation (**??**).

A final point of background concerns the relationship between the forces that drive fracture and the background ice flow. In real ice shelves, the state of stress is constantly evolving due to the change in geometry brought about by ice flow. Previous studies have examined the relationship between ice flow and fracture in several ways. **?** carried out viscous flow calculations to constrain the state of stress in their elastic calculations. They then tuned elastic moduli and boundary conditions in their elastic calculations to match the observed viscous stresses. **?** parameterized a state of stress from a viscous flow model, but rather than tuning elastic moduli instead chose to introduce fictitious equivalent body forces. Here, I consider the hypothesis that the forces that drive rift propagation are entirely described by the instantaneous ice shelf geometry and boundary conditions. This

hypothesis requires three-dimensional calculations in order to directly calculate –rather than parameterize or approximate– the role of gravitational driving forces. ~~I therefore continue to describe the details of a three-dimensional elastic fracture model.~~

2 ~~Mechanical Model~~

~~I begin this section by describing a~~ This paper is organized as follows. In Section 2, I describe three-dimensional ~~elastic model of an ice shelf in which stresses and displacements are calculated~~ elasticity calculations that are carried out using the finite element method ~~(Sections 2.1 and 2.2). I then describe a linear elastic fracture model which is closely related to these elasticity calculations (Section 2.3).~~ and then post-processed to reveal fracture mechanical properties. I present three-dimensional results in Section 3. These results motivate a simplified two-dimensional treatment in Section 4, the results of which are given in Section 5. I conclude by discussing the relationship between rift propagation, the compressive arch, rift-filling melange, and ocean swell in Section 6.

2 Three-dimensional model

2.1 Geometry

I consider the idealized ice shelf geometry shown in Fig. 1. The ice shelf is square in map view (the x-y plane). The z axis is defined so that the positive z axis points upwards and the bottom of the ice shelf is located at $z = 0$. The ice shelf has horizontal dimensions $L_x = L_y = 100$ km and thickness $h = 200$ m. The ice shelf surface at $y = 0$ faces the ocean and the surface at $y = L_y$ faces the ice sheet. The surfaces at $x = 0$ and $x = L_x$ are referred to as the ice shelf margins. A single rift is located along the x axis at $y = W$. I treat two different general rift locations: marginal and central. These two rift locations are shown in Fig. 2. I hold the rift length fixed at $L = 2.5$ km long for the marginal rift and $L = 5$ km long for the central rift.

Geometrically, I model a rift as a ~~tapered~~ rectangular hole in the ice shelf. Fractures in three dimensions have a fracture tip defined by a two-dimensional curve rather than a point. Although I refer to a rift tip for brevity, this term actually refers to a rift tip curve. In the treatment presented here, the rift tip curve is taken to be a vertical straight line. The rift is uniformly 10 m wide over most of its length. Simulations show ~~negligible~~ low sensitivity to the choice of this width ~~. Tapering is applied over a length equal to several widths (i.e., several tens of meters) near the rift tip~~(for example, stress intensity factors, described later, show changes less than or on the order of 1% change in response to changing the rift width to 15 m).

2.2 Linear elasticity

I consider the equations of linear, homogeneous, isotropic, static, three-dimensional elasticity (**?**),

$$\nabla \cdot \mathbf{T}' = -\rho \mathbf{g} \tag{1}$$

with total (Cauchy) stress tensor $\mathbf{T}'$, ice density ρ, and gravitational acceleration $\mathbf{g}$. Because I neglect any spatial variation in material parameters, my model does not include a firn layer.

I account for an initial hydrostatic stress in a manner following **?** wherein the equations of elasticity are solved for a perturbation stress tensor $\mathbf{T}$ defined as the total (Cauchy) stress tensor minus the initial ~~hydrostatic pressure,~~ overburden pressure,

$$\mathbf{T} \equiv \mathbf{T}' - p_0 \mathbf{I}, \tag{2}$$

with ~~,~~ identity tensor $\mathbf{I}$, overburden pressure

$$p_0 \equiv \rho g (H - z), \tag{3}$$

and ice sheet surface height H.

The perturbation stress tensor is necessary for the following physical reason. Without subtracting the initial overburden pressure, the ice shelf experiences an initial volumetric contraction $\sim p_0/K$ with bulk modulus K. This volumetric contraction does not occur in real ice shelves because at time scales longer than the Maxwell time, ice is well approximated as being incompressible (**?**). Note that the perturbation stress tensor is not equal to the deviatoric stress tensor defined as ~~$\mathbf{T}' - p\mathbf{I}$~~ $\mathbf{T}' - p\mathbf{I}$. This difference is important because the perturbation stress tensor accurately captures permissible, elastic volumetric contraction, whereas the deviatoric stress tensor does not.

~~All~~ The three-dimensional elasticity calculations in this study are carried out with respect to this perturbation stress tensor. ~~The~~

With respect to the perturbation stress tensor, the equations of motion are,

$$\nabla \cdot \mathbf{T} = 0 \tag{4}$$

$$T_{ij} = K\delta ij\epsilon_{kk} + 2\mu(\epsilon_{ij} + \delta_{ij}\epsilon_{kk}/3), \tag{5}$$

$$\epsilon_{ij} = \frac{1}{2}\left(\frac{\partial u_i}{\partial x_j} + \frac{\partial u_j}{\partial x_i}\right). \tag{6}$$

The first of these equations describes momentum balance which is derived by combining Eq. (2) and (3). Eq. (5) describes the elastic constitutive relation (Hooke's Law) with shear modulus $\mu = 3.6$ GPa and Poisson's ratio $\nu = 0.3$. Although isotropic elasticity only requires two elastic moduli, for convenience I use Young's modulus ~~$E = 2\mu(1+\nu)$~~ $E = 2\mu(1+\nu)$ and the bulk modulus $K = E/[3(1-2\nu)]$. Eq. (6) defines the strain tensor ϵ_{ij}. These equation use index notation with repeated indices implying summation, δ_{ij} denoting the Kronecker delta function, and the indices i, j taking values x, y, z.

2.2.1 Boundary conditions

The ice front, rift walls, and top and bottom ice shelf surfaces are loaded by a depth-varying normal stress that is equal to the water pressure below the waterline and equal to zero above the waterline. These boundaries have zero ~~applied~~ shear stress. The water pressure condition may be written as,

$$\mathbf{n}^T \cdot (\mathbf{T}' \cdot \mathbf{n}) = -p_w(z), \tag{7}$$

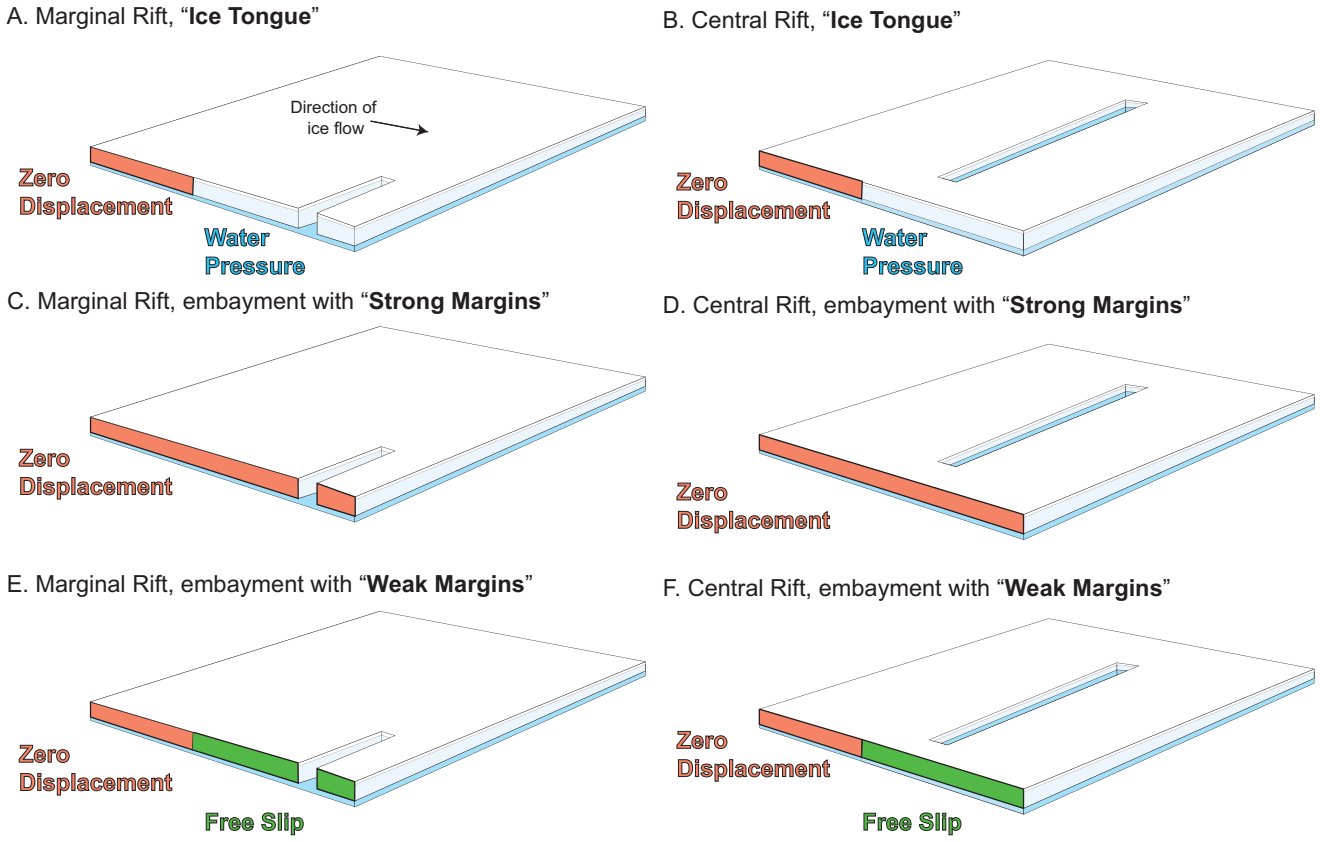

Figure 2. The geometries and boundary conditions considered in this study~~include~~: A. and B., ~~Half zero displacement and half water pressure conditions~~Ice tongue; C. and D., ~~entirely zero displacement conditions~~strong margins; and, E. and F., ~~half~~ zero displacement~~and half free slip conditions~~. ~~I furthermore consider rifts that occur in the margins (~~A., C., and E. ~~) and central~~ show marginal rifts ~~(~~and B., D., and F. ~~)~~show central rifts. The figures are not drawn to scale~~and the rift width is greatly exaggerated~~.

with unit outward pointing normal vector $\mathbf{n}$, ice shelf draft ~~$H_w = \rho/\rho_w h$,~~ $H_w = \rho/\rho_w h$, ice and water densities ρ and ~~water pressure $p_w(z)$,~~ ρ_w, and water pressure,

$$p_w(z) \equiv \begin{cases} \rho_w g\left[H_w - (z + u_z)\right] & z < H_w, \\ 0 & z \geq H_w. \end{cases} \tag{8}$$

~~Here, w is the vertical component of the displacement vector.This boundary condition~~

The boundary conditions applied in the three dimensional model are found by combining Eqs. 2, 7, and 8. This approach is consistent with previous treatments of crevasse propagation in glaciers (e.g., **?**).

In all simulations~~that are presented here~~, the surface of the ice shelf above the grounding line at $y = L_y$ has a zero displacement boundary condition. Similarly, the ice shelf surface at the ice front at $y = 0$ has a water pressure boundary condition (Eq. 8). In the margins, I examine three types of marginal boundary condition. These conditions are shown in Fig. 2; they are:

1. Ice shelf with ice tongue: margins have zero displacement between $y = L_y/2$ and $y = L_y$ and have water pressure between $y = 0$ and $y = L_y/2$;
2. Ice shelf in an embayment with strong margins: margins have zero displacement boundary condition; and,
3. Ice shelf in an embayment with weak margins: margins have zero displacement between $y = L_y/2$ and $y = L_y$ and have zero shear stress and zero normal displacement between $y = 0$ and $y = L_y/2$.

~~Note that Equations 18-20 occur naturally as a result of the more general three-dimensional boundary conditions. Equations 18-20 are not applied as constraints in the three-dimensional calculations. They are used, however, in Section 4 to analytically approximate the numerical results.~~

2.2.2 Numerical implementation

I solve Eqs. 4-6 using the finite element method. The ice shelf domain is discretized using a free ~~tetrahedral mesh in three spatial dimensions or a free triangular mesh in two spatial dimensions. In the three-dimensional simulations, the~~ (i.e., not regularly spaced) tetrahedral mesh. The maximum element size along the rift is ~~set to be $m = h/16$~~$h/16$. The element size then increases away from the rift to a maximum value of 3.5 km. The rift is geometrically formed as a rectangular prism with width $W_{\text{rift}} = 10$ m and length L. ~~I have verified that the~~ The results presented here have ~~virtually no~~ minimal dependence on the choice of W_{rift}~~and m. In the two-dimensional simulations (described below), the maximum element size along the rift is $W_{\text{rift}}/10$~~.

2.3 Linear elastic fracture

Fractures in elastic materials create displacement fields that vary proportional to the distance r from the crack tip as $r^{1/2}$ (**?**). The scalar constant of proportionality involves the stress intensity factor. Specifically, in terms of the displacement components u, v, and w corresponding to displacements in the x, y, and z directions, the stress intensity factors are defined through the relations (**?**),

$$u(r,z) = 4\frac{K_{II}(z)}{\mu/(1-\nu)}\sqrt{\frac{r}{2\pi}}, \tag{9}$$

$$v(r,z) = 4\frac{K_{I}(z)}{\mu/(1-\nu)}\sqrt{\frac{r}{2\pi}}, \tag{10}$$

$$w(r,z) = \frac{K_{III}(z)}{\mu}\sqrt{\frac{r}{2\pi}}. \tag{11}$$

The quantities K_I, K_{II}, and K_{III} are the Mode-I, Mode-II, and Mode-III stress intensity factors (SIFs). The sense of motion associated with each mode of fracture is shown in Fig. 3. Equations 9-11 represent the asymptotic value, accurate to first order,

of the displacement field near the rift tip on the plane of the fracture. The stress intensity factors bear a direct relationship to fracture propagation.

A basic tenet of fracture mechanics is that unstable crack growth occurs when the elastic strain energy available to drive fracture exceeds the energy required to create new fracture area (**?**). The key insight of linear elastic fracture mechanics is that this energy condition can be related to the stress intensity factors (**?**). The stress intensity factors may therefore be used as part of a fracture criterion. In this study, I examine mixed-mode fracture and I therefore use the theory of **?** that calculates the single optimally-oriented stress intensity factor from the three different stress intensity modes. This optimally-oriented stress intensity factor is the Mode I stress intensity factor along a plane oriented to minimizes K_{II} and K_{III} (**??**). Under the assumption (verified later) that K_{III} does not substantially contribute to the direction of propagation of the rift tip line, the Mode I stress intensity factor along the optimal angle of propagation θ can be written as,

$$K_I^{Op} \equiv \cos\left(\frac{\theta}{2}\right)\left[K_I \cos^2\left(\frac{\theta}{2}\right) - \frac{3}{2}K_{II}\sin\theta\right]. \tag{12}$$

In this expression, the angle of propagation θ is given by,

$$\theta \equiv -2\tan^{-1}\left[\frac{-2K_I + 2\sqrt{K_I^2 + 8K_{II}^2}}{8K_I I}\right]. \tag{13}$$

In the adopted sign convention, negative angles indicate the direction pointing away from the ice front and straight-ahead propagation occurs when $\theta = 0$. Note that care must be taken in selecting the correct quadrant for the $\tan^{-1}$ function.

The fracture propagation criteria may then be stated as,

$$K_I^{Op} > K_{Ic}, \tag{14}$$

where the value $K_{Ic} = 100$ kPa$\sqrt{\text{m}}$, is the Mode I fracture toughness of ice (**?**). I refer to rifts that satisfy Eq. (14) as being unstable because they are expected to undergo some amount of propagation. Note that this does not necessarily mean that the rift will propagate in a way that will lead to a calving event. Propagation may stop, for example, before calving occurs. Rifts that do not satisfy Eq. (14) will be referred to as stable; such rifts are expected to close. ~~This closure may result in partial contact of the rift walls, as discussed next.~~

2.3.1 Partial contact of rift walls

The partial contact of rift walls is a nonlinear phenomenon because it involves solving for the shape of the contacting region and therefore changing the region over which different boundary conditions are applied (**?**). Here, I treat a linear formulation of this problem wherein the Mode-I stress intensity factor K_I can take on positive or negative values. This situation is discussed in detail by **?**. For fractures with zero initial width, a negative K_I implies unphysical material overlap. I avoid this situation in my numerical simulations by giving the rift an initial nonzero opening as described in Section 2.1. This is consistent with the idea that rifts in ice shelves are probably not held open entirely by elastic stresses because they have deformed through creeping flow. Other studies have shown that accounting for contact nonlinearity results in minimal differences from the linear

problem for long fractures with $L \gg \lambda$ (**?**), where λ is the ice shelf flexural wavelength ~~.~~(discussed later, see Eq. 22). Given that many rifts do reach lengths $L \gg \lambda$ (**??**), the linear approximation may well prove adequate for many cases of glaciological interest.

2.3.2 Stress intensity factor calculations

~~Stress~~ The stress intensity factors are calculated ~~using rift wall displacements and Equations~~by solving Eqs. 9-11 numerically at an arbitrary distance r from the crack tip. This evaluation method, essentially a post-processing step, is sometimes called the displacement correlation method (**?**) and has previously been used in glacier studies by **?**. I evaluate Equations 9-11 at a distance r from the crack tip that is at least several times ~~m~~ the grid spacing in order to achieve grid-size independence. In three dimensions, stress intensity factors are calculated at various heights through the ice shelf thickness, with the resulting calculations plotted in Fig. 3.

3 Results ~~and Analysis~~from three-dimensional model

Fig. 3 shows a typical result of the finite element calculations. This figure shows that the Mode-I and Mode-III stress intensity factors are nearly linear with depth (i.e., Fig. 3A, B, and E), while the Mode-II stress intensity factor is nearly uniform with depth (i.e., Fig. 3D). ~~This structure in the solutions permits an approximate parameterization of three-dimensional effects. Such a parameterization allows for a much less computationally costly, two-dimensional problem to be solved.~~

~~I next develop the analytical parameterization (Section 4). After developing this 2D parameterization, I then apply it to examine the relationship between rift position and rift stability. Some readers may wish to skip directly to these results, which are given in Section 5.2.~~

3.1 ~~Parameterization of 3D effects within 2D calculations~~

~~The~~ Empirically, the structure of the three-dimensional stress intensity factors ~~suggests the approximation~~can be described as,

$$K_I(z) = K_I^m + K_I^b \left(\frac{z - h/2}{h/2} \right), \tag{15}$$

$$K_{II}(z) = K_{II}^m, \tag{16}$$

$$K_{III}(z) = K_{III}^b \left(\frac{z - h/2}{h/2} \right), \tag{17}$$

where the superscripts b and m stand for bending and membrane, respectively. ~~In the following , I calculate the bending components of the stress intensity factors K_I^b and K_{III}^b analytically and the membrane components K_I^m and K_{II}^m using~~ This observed structure motivates the following parameterized, two-dimensional ~~finite element solutions.~~ treatment.

~~Comparison between 2D and 3D calculations$h$ 2D 3D m (2D-3D)/3D χ 100 m -0.2937 -0.3127 12.5 m -6.1% 200 m -0.2937 -0.3012 5 m -2.5%200 m -0.2937 -0.3069 12.5 m -4.3%ψ 100 m-0.04408-0.0385 12.5 m +14.5%200 m -0.04408 -0.0382 5 m +15.4%200 m -0.04408 -0.0379 12.5 m +16.3%~~

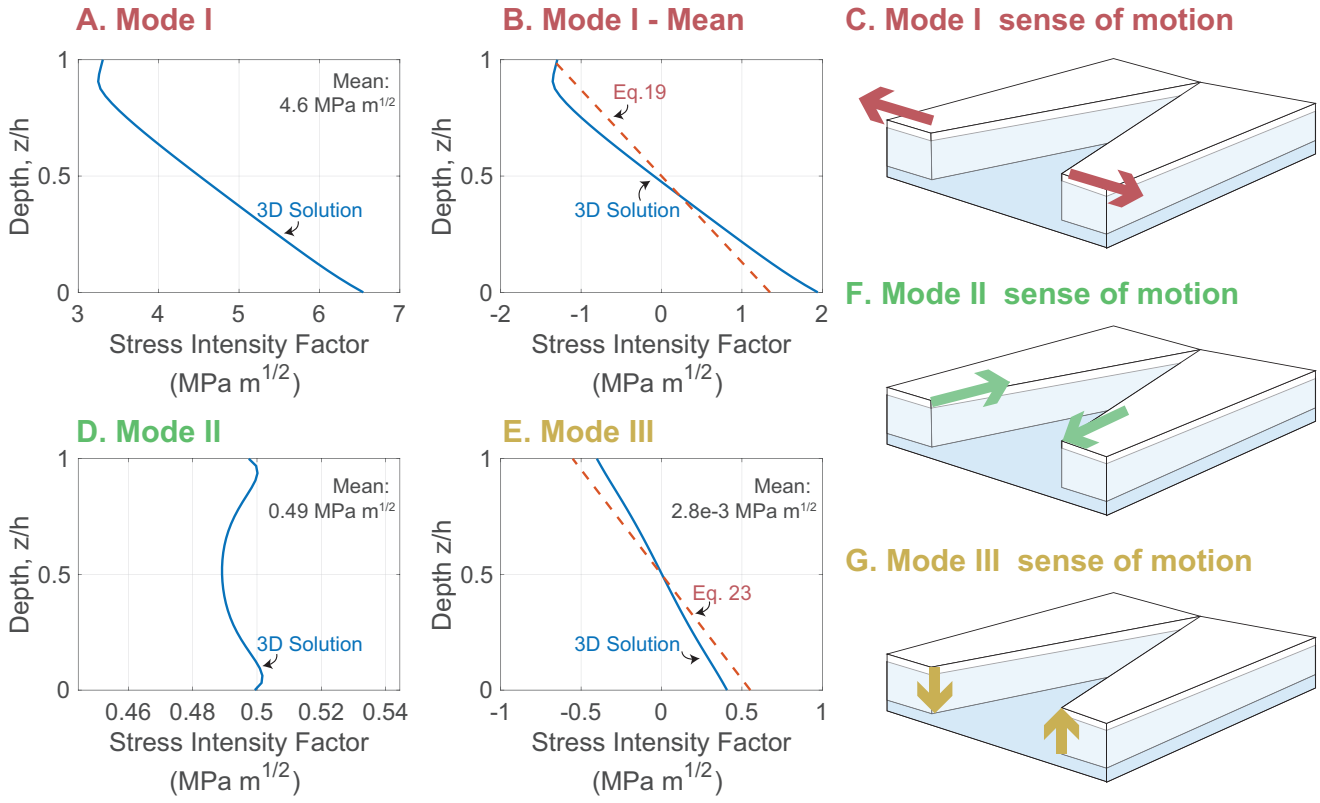

Figure 3. Typical three-dimensional stress intensity factors (SIFs) as a function of depth z in the ice shelf. The particular SIFs are for a marginal rift in an ice tongue (Fig. 2A). ~~and B~~A. ~~show the~~ Mode I stress intensity factor ~~K_I~~(SIF), B. Mode I SIF with depth-mean removed, C. Mode I sense of motion, D. ~~shows the~~ Mode II ~~stress intensity factor K_{II} and~~ SIF, E. ~~shows the~~ Mode III ~~stress intensity factor K_{III}~~ SIF, F. ~~The associated~~ Mode II sense of ~~motion for each mode is shown in panels C~~Motion, ~~F, and~~ G. ~~B~~Mode III sense of motion. ~~has~~ Red dashed lines show the ~~mean removed and is compared to the analytical solution~~ simplified model of ~~Eq.~~Section ~~(19)~~4. ~~The particular stress intensity factor solutions in these figures are plotted for a marginal rift in an ice tongue (i.e., the geometry shown in Fig. 2A.~~

4 Two-dimensional model

I now examine a parameterized two-dimensional model with the goal of approximating Eqs. 15-17. The membrane terms in these equations are calculated numerically by solving the equations of plane strain elasticity in two horizontal spatial dimensions x and y. The governing equations for the two-dimensional calculations are found by taking $\partial/\partial z = 0$ in Eqs. 4-6. The two-dimensional finite element calculations are similar to the three-dimensional ones, with tetrahedral elements being replaced by triangular ones and a minimum mesh size $W_{\text{rift}}/10$. Boundary conditions are chosen, as in the three-dimensional calculations, to be either freely slipping, to have zero displacement, or to have an applied traction that represents an ice front. The latter is given by the classical ice front membrane stress solution of **?**,

$$\sigma_m = \frac{\rho g h}{2}\left(1 - \frac{\rho}{\rho_w}\right). \tag{18}$$

Note that this boundary condition is simply the depth integrated water pressure minus overburden pressure as given in Eq. 7-8.

4.0.1 ~~The bending components of the SIFs~~

Bending terms, in contrast, are parameterized in the two-dimensional treatment. I find that the bending ~~component of the Mode-I stress intensity factor~~ contribution to the opening mode is well fit by the ~~previously-published~~ stress intensity factor solution ~~(????),~~ **(?)**,

$$K_I^b = -\sigma_b f(\nu)\sqrt{\lambda}, \tag{19}$$

~~Here, $\lambda^4 = D/(\rho g)$ is the flexural length~~ with bending stress **(?)**,

$$\sigma_b = \frac{6 m_0}{h^2} = \phi \frac{\rho g h}{2}. \tag{20}$$

The bending stress σ_b is the value of the rift-normal stress at the top of the ice shelf; it is also the maximum value of the rift-normal stress. The bending stress can be expressed as a bending moment,

$$m_0 \approx \frac{\rho g h^3}{12}\left[3\left(\frac{\rho}{\rho_w}\right) - 2\left(\frac{\rho}{\rho_w}\right)^2 - 1\right] = \phi \frac{\rho g h^3}{12}. \tag{21}$$

Typical values of $\rho/\rho_w = 0.90$ give $\phi = 0.08$. In addition, Eq. 19 makes use of the flexural gravity parameter,

$$\lambda^4 = D/(\rho g), \tag{22}$$

with flexural rigidity ~~$D = Eh^3/[12(1-\nu^2)]$~~ $D = Eh^3/[12(1-\nu^2)]$. Hence, flexure results in a stabilizing contribution to the Mode I stress intensity factor that grows with ice thickness according to $K_I^b \sim h^{11/8}$. The ~~bending stress σ_b is given by Eq. (20). The~~ function $f(\nu)$ is discussed below. Notably, the bending stress intensity factors asymptotically vary with $\sqrt{\lambda}$ instead of the typical $\sqrt{L}$.

There is some discrepancy in the literature concerning the precise values of the function $f(\nu)$. **?** cites **?** who both note that f is of order unity but do not give its exact form. **?** appears to have first given the dependence of f on ν although **?** found a mistake in this work. Meanwhile, **?** gives a different value of f. It appears, however, that **?** did not correctly account for the rift-wall boundary condition. Given this uncertainty and the additional detail involved in the three-dimensional problem beyond the assumptions made by the above authors, I instead simply choose to calculate the value of $f(\nu)$ from the three-dimensional calculations. From these calculations, I find a value $f(\nu = 0.3) = 0.7646$. Of the above references, this value is most similar to the value calculated from the equation given by **?**, $f(\nu = 0.3) = 0.6063$.

Bending also creates a Mode-III stress intensity factor. Assuming that this bending can also be described within Euler beam theory, the Mode-III and Mode-I stress intensity factors are related by a factor,

$$\frac{K^b_{III}}{K^b_I} = \frac{h}{2\sqrt{2}(1+\nu)\lambda}. \tag{23}$$

Thus $K^b_{III} \sim h^2$, which is a larger exponent than for K^b_I. This solution was derived by assuming, consistent with Equations 9-11, that the ratio of stress intensity factors is proportional to the ratio of the stresses. This stress ratio is then calculated using the solution to the floating beam equation (**?**), $w = -2m_0/(\rho g \lambda^2)\exp(-x/\lambda)(\cos y/\lambda - \sin y/\lambda)$. The analytical solution of Eq. (23) is compared to the finite element solution in Fig. 3E (red dashed lines).

5 Results from two-dimensional model

5.1 Comparison between 2D and 3D

I find good agreement between two-dimensional calculations and the depth-averaged values from three-dimensional calculations. Table 1 presents these results using the geometrical factors $\chi = K^m_I/(\sigma_m\sqrt{\pi L})$ and $\psi = K^m_{II}/(\sigma_m\sqrt{\pi L})$, where σ_m is the depth-integrated boundary condition given in Eq. (18). Note that $K_I \sim K_{II} \sim \sqrt{L}$ suggests that χ and ψ do not depend on L (**?**). The agreement is better for χ than for ψ, with differences on the order of several percent. This table also shows the effect of varying the maximum near-tip element length. The values in this table are calculated for a central rift in an embayment with strong margins (i.e., as shown in Fig. 2D).

The analytical solution is not expected to perfectly match the finite element solution because the latter accounts for the full floatation condition (Eq. 7), whereas the bending model (Eq. 19) neglects higher order moments through Eq. (21). I further verify that the simplified model captures the behavior of the three-dimensional simulations by calculating stress intensity factors over a range of ice shelf thickness between 25 m and 1600 m. I find that $K^b_I \sim h^{1.31}$ in the three-dimensional calculations whereas $K^b_I \sim h^{1.375}$ analytically. Similarly, $K^b_{III}/K^b_I \sim h^{0.27}$ in the three-dimensional calculations whereas $K^b_{III}/K^b_I \sim h^{0.375}$ analytically. As can be seen in Fig. 3, the differences are more pronounced for K^b_{III}. I attribute the differences between analysis and calculation to the neglect of higher order moments and stress terms (i.e., the use of Euler beam theory).

5.1.1 ~~The membrane components of the SIFs~~

Table 1. Comparison between 2D and 3D calculations

	h	2D	3D	Max. near-tip element size	(2D-3D)/3D
χ	100 m	-0.2937	-0.3127	12.5 m	-6.1%
	200 m	-0.2937	-0.3012	5 m	-2.5%
	200 m	-0.2937	-0.3069	12.5 m	-4.3%
ψ	100 m	-0.04408	-0.0385	12.5 m	+14.5%
	200 m	-0.04408	-0.0382	5 m	+15.4%
	200 m	-0.04408	-0.0379	12.5 m	+16.3%

~~I carry out simplified two-dimensional finite element calculations in order to describe the membrane components of the stress intensity factors. In two horizontal spatial dimensions x and y, the governing equations for the two-dimensional calculations are found by taking $\partial/\partial z = 0$ in Eqs. 4-6. In two spatial dimensions, the boundary condition on floating ice fronts takes the stress value given by Eq. (18).~~

~~I find good agreement between two-dimensional calculations and the depth-averaged values from three-dimensional calculations. Table 1 presents these results using the geometrical factors $\chi = K_I^m/(\sigma_m\sqrt{\pi L})$ and $\psi = K_{II}^m/(\sigma_m\sqrt{\pi L})$, where σ_m is the depth-integrated boundary condition given in Eq. (18). Note that $K_I \sim K_{II} \sim \sqrt{L}$ suggests that χ and ψ do not depend on L (?). The agreement is better for χ than for ψ, with differences on the order of several percent. This table also shows the effect of varying the maximum near-tip element length m. The values in this table are calculated for a central rift in an embayment with strong margins (i.e., as shown in Fig. 2D).~~

5.2 ~~Central and~~ Marginal and Central Rifts

I ~~now~~ use the two-dimensional approach described in Section 4 to examine the effect of rift position on rift stability. I ~~again consider all of the~~ consider all combinations of boundary conditions and rift locations shown in Fig. 2 while additionally varying the streamwise position of the rift W.

Stress intensity factors for marginal rifts are plotted in Fig. 4. ~~These stress intensity factors were calculated using the 2D parameterization described in Section 4.~~ Consistent with the shearing stresses experienced in the ice shelf margins, the Mode I and Mode II stress intensity factors are of similar magnitude (Fig. 4A and B, respectively). ~~Fig. 4C shows that marginal rifts always tend to propagate in the direction~~ In all marginal rift simulations, rifts propagate away from the ice front ~~, i.e., in the positive y direction (coordinates shown in~~ (Fig. ~~1).~~ 4C). Marginal rifts are unstable over the greatest range of locations in the ice tongue and weak margin geometries (Fig. 4D). ~~Specifically, they become unstable at a position $W/L_y \approx 0.66$. Stability in these geometries is not spatially monotonic, however, and rifts again become stable near the ice front at $W/L_y \approx 0.33$.~~ In both cases, rifts are unstable at positions $0.35 < W/L_y < 0.65$. Marginal rifts in ice shelves with strong margins, in contrast, ~~have monotonically varying optimally~~

~~oriented Mode I SIFs: they~~ are stable near the grounding line and they become unstable at a distance $W/L_y \approx 0.33$ from the ice front.

Stress intensity factors for central rifts are plotted in Fig. 5. In contrast to ~~the~~ marginal rifts, central rifts have $|K_{II}| \ll |K_I|$ (Fig. 5A and B). Unlike marginal rifts, propagation angles are smaller, indicating nearly straight-ahead propagation (Fig. 5C). ~~Furthermore, central~~ Central rifts in all positions are found to have negative optimally oriented stress intensity factors indicative of stability (Fig. 5D).

6 Discussion

I have presented a three-dimensional LEFM analysis of ice shelf rift propagation. While this model has many potential applications, I have focused on the relationship between ~~rift position~~ marginal strength and rift stability. In that regard, the main result of this analysis is that rifts originating in the margins of ice shelves become unstable if the ice shelf margin looses shear strength. This transition between a strong margin and a weak margin can be seen, for example, by comparing the red and yellow curves in Fig. 4D. Although this result is justified by the calculations presented in this paper, it is worth emphasizing several ~~implicit and subtle~~ assumptions.

I have assumed that margins have either zero displacement or zero shear stress. In reality, margins likely experienced reduced but nonzero shear stress. I have also considered only two rift locations (marginal or central), only one ice shelf geometry (square), and only one rift geometry (a single rift, perpendicular to flow, and without curvature). I treat the entire ice column as having ~~identical~~ uniform material properties and therefore ~~do not describe the firn layer and~~ describe neither a firn layer nor its relation to partial contact of rift walls. Additional observed rift-wall processes such as brine infiltration, surface accumulation, and variable uplift could also be investigated (**???**). Each of these assumptions deserves further examination. Despite these limitations, ice shelves and ice shelf rifts oftentimes approximately conform to the assumptions described in this study. I do therefore expect that the results presented here provide a useful basis for understanding rift propagation.

6.1 The compressive arch

All boundary conditions considered here give rise to a compressive arch, defined as the region where an ice shelf transitions from uniaxial to biaxial extension ~~(?). The compressive arch can be visualized by plotting the second principle horizontal strain field, the first principle strain alway being positive~~ (Fig. 6). **?** proposed the hypothesis that "once a retreating ice front breaks through the critical 'compressive arch' then retreat is irreversible." ~~The~~ Although the results presented here broadly confirm a connection between the compressive arch and rift propagation, there are important caveats. The foremost exception to the compressive arch hypothesis is that central rifts are found to always be stable, regardless of their position inside or outside of the ~~hypothesis of ?, although as shown in Section 3, the relation to the~~ compressive arch~~only holds in an approximate sense. Specifically~~. Additionally, for the strong margin boundary condition the onset of instability occurs somewhat upstream from the maximum extent of the compressive arch~~(~~. This is shown in Fig. 6A.~~)~~, where the compressive arch is plotted as a black dashed line and marginal stability boundaries are plotted with yellow dashed lines. For the weak margins and ice tongue

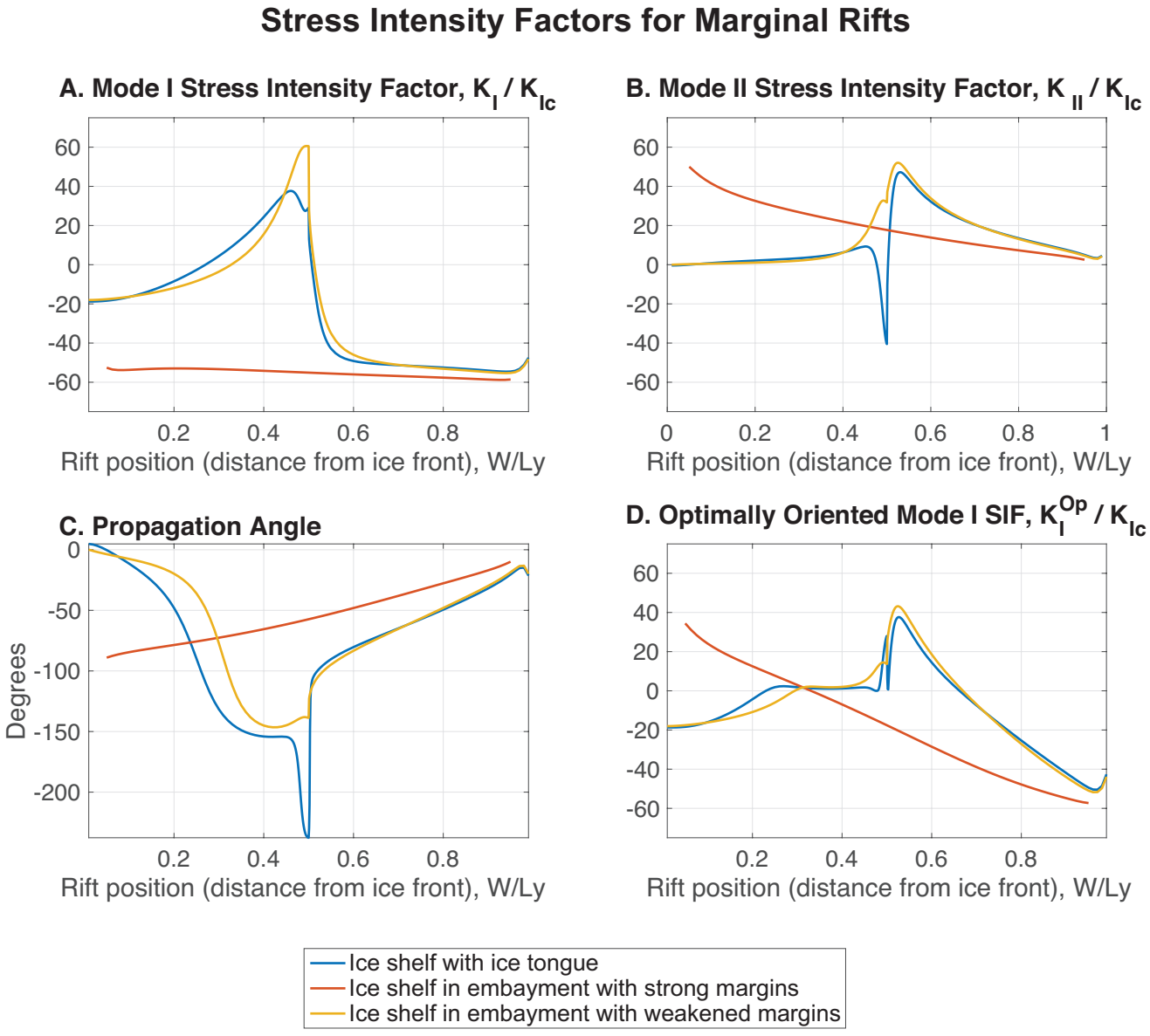

Figure 4. Stress intensity factors for marginal rifts may reflect either stability or instability depending on the position of the rift. Three pieces of information, the A. Mode I SIF, B. Mode II SIF, and C. Propagation angle, are combined using Eq. (12) to calculate D. the optimally-oriented SIF.

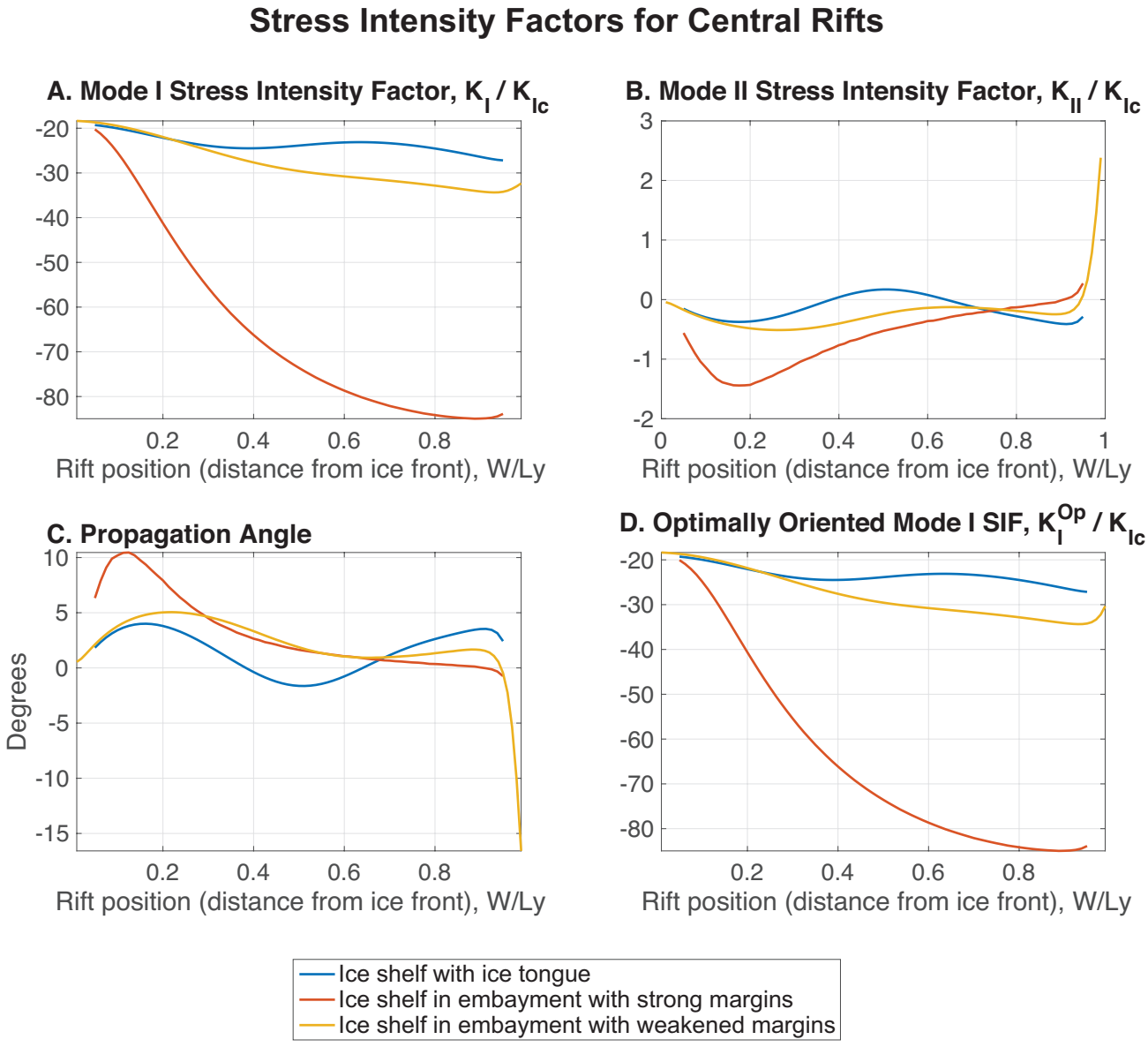

Figure 5. ~~Stress intensity factors~~ Same as Fig. 4 but for central rifts~~reflect stability for all rift positions. Three pieces of information, the A. Mode I SIF, B. Mode II SIF, and C. Propagation angle, are combined using Eq. (12) to calculate D. the optimally-oriented SIF.~~

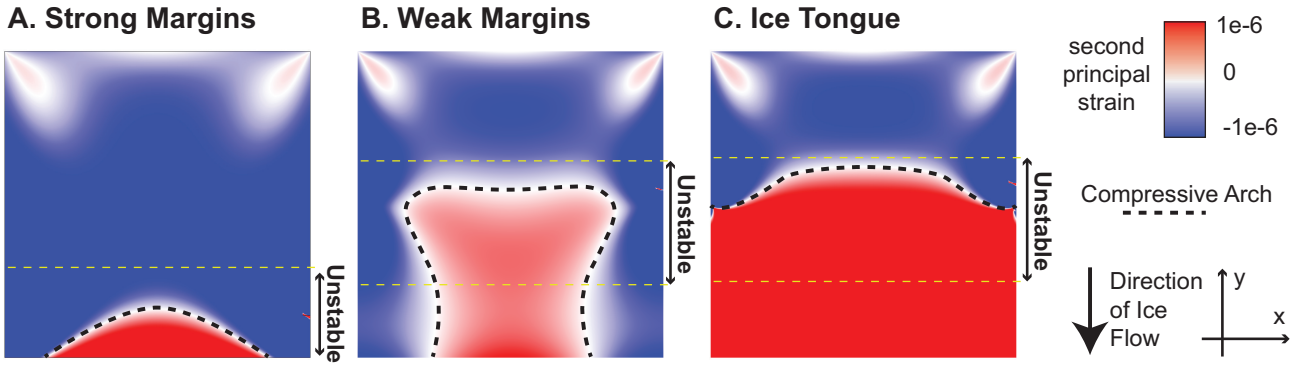

Figure 6. The ice shelf compressive arch (thick black dashed line) is plotted for three boundary conditions: A. Strong Margins, B. Weak Margins, and C. Ice Tongue (see Fig. 2). The figure also shows the boundaries of regions of ~~rift~~ instability for marginal rifts (thin yellow dashed lines). These figures were calculated in two horizontal spatial dimensions as described in Section ~~??~~4.

boundary conditions the agreement is closer, however, there is also a region of stability that occurs closer to the ice front (Fig. 6B. and C.).

~~Perhaps more~~ Perhaps most importantly, the results presented here suggest a slightly different order of causality than that proposed by **?**. ~~Rather than being an independent~~ In the hypothesis of **?**, the compressive arch is a boundary that rifts may or may not propagate through~~, rift propagation in the model presented here is expected to occur precisely because of the stress state that creates the compressive arch . Ice shelf retreat is expect to be irreversible only~~ . The present analysis instead suggests that a rift "propagating across the compressive arch," actually involves simultaneous changes in ice geometry, migration of the compressive arch, and rift propagation. Under the assumptions of my analysis, calving of icebergs within the compressive arch is only reversible insofar as marginal weakening is ~~itself~~ irreversible.

6.2 Melange as a rift proppant

? observed a lack of rift-tip seismicity at central rift in the Ross Ice Shelf. This observation is qualitatively consistent with the negative K_I^{Op} I have calculated for centrally-located rifts. ~~In the absence of other forces such rifts~~ A negative stress intensity factor indicates a rift that will tend to close. It seems likely that these rifts therefore owe their continued existence to rift-filling melange that acts as a type of proppant by holding the rift open. Melange therefore has a dual nature. **?** and **?** showed that melange maintains shear stresses and therefore resists viscous flow. In this sense, melange is stabilizing. Yet in the sense that melange may sometimes enable the existence of rifts that would otherwise close, melange is destabilizing.

6.3 Wave-induced fracture

? used passive seismic data to calculate the elastic ice shelf stresses due to ocean swell acting on the Ross ice shelf. This study concluded that some un-modeled process must have been operating in order to explain the lack of any observed ice shelf rift

propagation during the observation period. Specifically, **?** calculated a maximum wave-induced Mode-I stress intensity factor $K_I \approx 2$ MPa m$^{1/2}$ for a site near the Nascent Iceberg Rift. Using the results presented here for a central rift, we calculate that for a near-front central rift with $W/L_y = 0.05$, the Mode-I stress intensity without wave stress would be $K_I^{Op} \approx -5$ MPa m$^{1/2}$. The resulting total Mode-I stress intensity factor of $K_I^{Op} \approx -3$ MPa m$^{1/2}$ being negative is consistent with the observation that ocean swell did not trigger rift propagation during the observation period described by **?**.

7 Conclusion

I have modeled an ice shelf as a three-dimensional buoyantly floating elastic plate. I then show how these three-dimensional results may be captured in simplified two-dimensional calculations. Using the two-dimensional theory, I show that ice shelf rifts become unstable in the presence of marginal weakening or upon exiting an embayment. These results are a step towards ~~prognostic ice shelf modeling~~ modeling marine ice sheet evolution with a physics-based relationship between ice ~~dynamics~~ flow and an ice ~~front~~ extent set by rift propagation.

Code and data availability. The analysis code used in the text is available on the author's GitHub repository.

Competing interests. The author declares that no competing interests are present.

Acknowledgements. This project began with a discussion with Colin Meyer at the Cambridge symposium of the International Glaciological Society in 2015. Jim Rice and Eric Dunham read earlier versus of this manuscript and gave ~~the author~~ helpful comments. Several discussions with Brent Minchew, Jan De Rydt, and Hilmar Gudmundsson also ~~helped~~ provided interesting feedback along the way. On a visit to C.U. Boulder organized by Jed Brown, David Marshall was critical of some early results; this feedback was helpful. The author was funded by the Department of Earth and Planetary Sciences at Harvard University.